# Quasiunique amplitude for $I=0$ $KN$ scattering below 1.89 GeV in center-of-mass system and implications for bag models

M. J. Corden, G. F. Cox, D. P. Kelsey,* C. A. Lawrence, and P. M. Watkins
*Department of Physics, University of Birmingham, Birmingham, United Kingdom*

O. Hamon, J. M. Lévy, and G. W. London†
*Laboratoire de Physique Nucléaire et de Hautes Énergies, Paris, France*
(Received 20 July 1981)

Quasiunique results are presented of an energy-dependent partial-wave analysis of $I=0$, $KN$ scattering between 1.47 and 1.89 GeV in c.m. system. The data set used incorporates new results on the reaction $K_L^0 p \to K_S^0 p$ and new polarization measurements in $K^+ n$ elastic and charge-exchange scattering as well as $K^+ n$ elastic and charge-exchange differential cross sections. A careful analysis of the input hypotheses, notably the effects of different parametrizations with their different theoretical or phenomenological assumptions, is made. No obvious evidence is found for any exotic classical positive-strangeness baryon resonance. However, there is evidence for poles in the $P$ matrix for both $I=0$ and $I=1$, corresponding to confined quark states of bag models. Some predicted states are unobserved and an unpredicted state in $I=1$, $S_1(1.786$ GeV), is observed.

## I. INTRODUCTION

The phenomenological constituent quark model, the Isgur-Karl model[1] for example, has had many successes in predicting observed hadron states and properties, and in addition, the nonexistence of exotic states. On the other hand, other models, for example the color chemistry inspired by QCD theory, predict a much richer spectrum of hadron states. In particular in the MIT bag model[2] where confinement is imposed, Jaffe[3] has shown that exotic mesons $|q^2\bar{q}^2\rangle$ and exotic baryons $|q^4\bar{q}\rangle$ are predicted on the same basis as ordinary hadrons $|q\bar{q}\rangle$ and $|q^3\rangle$. The nonobservance of these states remains an enigma which is perhaps resolved by the introduction by Jaffe and Low[4] of the $P$ matrix which connects the predicted quark states within the bag with the hadron scattering states measured outside the bag; a pole in the $P$ matrix would indicate the existence of the discrete quark state.

A clear test of these various models is to be found in $Z$ states, that is, in $I=0$ and $I=1$ $KN$ scattering where various $Z_1$ and $Z_0$ states are predicted by bag (or string) models[5] (see Table I).

$I=1$ $KN$ scattering has been studied in various phase-shift analyses[6–8] using $K^+p$ total and inelastic cross sections and $K^+p$ elastic and inelastic differential cross sections as well as polarization data.

TABLE I. Predictions of de Swart *et al.* (Ref. 5) for masses (in GeV/$c^2$) of exotic states and poles of $P$-matrix analysis (see Sec. III).

| | Ref. 5 | | $P$-matrix analysis | |
|---|---|---|---|---|
| Wave | $Z_0$ | $Z_1$ | $Z_0$ | $Z_1$ |
| $S_1$ | 1.700 | 1.900 | 1.690 | 1.786 |
| | | | | 1.950 |
| $P_1$ | 1.720 | 1.870 | 1.720 | 1.823 |
| | 1.870 | 1.910 | | |
| $P_1$ | 1.720 | 1.870 | 1.900 | 1.788 |
| | 1.870 | 1.910 | | |

 

The three analyses result in qualitatively similar partial waves but differ in interpretation, perhaps due to different parametrizations. The analyses in Refs. 6 and 7 agree that there are no classical resonances in any wave for masses up to 1900 MeV/$c^2$ while the analysis in Ref. 8 with a larger data base claims a classical resonance in the $P_3$ wave at $M=1796$ MeV/$c^2$ and $\Gamma=101$ MeV/$c^2$. A complication arises naturally in these analyses due to inelastic channels $K\Delta$ and $K^*N$.

$I=0$ $KN$ scattering has been studied in two phase-shift analyses[7,9] using $I=0$ total and inelastic cross section and $K^+n$ elastic and charge-exchange differential cross sections. The analysis in Ref. 9 resulted in three families of solutions, labeled A, C, and D; the latter solution shows resonancelike behavior in the $P_1$ wave. With a different parametrization and a larger data sample *and* excluding *a priori* the A-type solution without any statistical justification, the analysis in Ref. 7 resulted in a solution somewhat similar to C, claiming no classical resonance interpretation. However, Roiesnel,[10] using the results of this analysis, claims a $P$-matrix pole in the $S_1$ wave.

Since these analyses were performed, qualitatively new data with good statistics bearing on the $Z_0$ amplitude have become available, in particular in the $K_L^0p\rightarrow K_S^0p$ channel,[11–13] and polarization measurements in the $K^+n$ elastic and charge-exchange reactions.[14,15] *It is important to emphasize that these new data are not properly predicted by the analysis in either Ref. 7 or Ref. 9 and thus a new and complete analysis is necessary.*

We present in this paper a new and complete phase-shift analysis of the $Z_0$ amplitude using all relevant data and treating with great care the problems of particular parametrizations in order to isolate the parametrization-independent characteristics. Section II describes this analysis and presents the solution whose features are quasi-independent of input assumptions, in particular the parametrization. Section III presents a discussion of the $Z_1$ and $Z_0$ amplitudes within the $P$-matrix formalism.

## II. $Z_0$ PARTIAL-WAVE ANALYSIS

### A. Data used in the analysis

The following types of data have been used in the analysis: the $I=0$ total and inelastic cross sections, differential cross sections for the reactions

$$K^+n(p)\rightarrow K^+n(p)\ , \tag{1}$$

$$K^+n(p)\rightarrow K^0p(p)\ , \tag{2}$$

$$K^0p\rightarrow K^+n\ , \tag{3}$$

$$K_L^0p\rightarrow K_S^0p \tag{4}$$

and polarizations for the first two reactions. A complete list including references and momenta is given in Table II. In general the data set contains the most recent and high-statistics data. In particular, where the total-cross-section measurements overlap, only the more recent data with better statistical accuracy have been used. The choice of 1.2 GeV/$c$ laboratory momentum as the upper limit of the analysis was greatly influenced by the energy range of the $K_L^0$ and polarization data now available.

The forward real parts of the $Z_0$ scattering amplitude calculated in Ref. 7 were not included in the fit since a proper statistical treatment is not possible; however, the final fit reproduces these predictions satisfactorily.

### B. Treatment of deuterium data

Previous determinations of $Z_0$ were based solely on data from the elastic (1) and charge-exchange (2) reactions. Ideally the amplitudes for these reactions are $\frac{1}{2}(Z_1+Z_0)$ and $\frac{1}{2}(Z_1-Z_0)$, respectively. However the fact that the data are taken with a deuterium target necessitates the introduction of so-called form factors which relate the measured angular distributions to the scattering amplitudes.

The form factors used in the present analysis are based on the theoretical work of Alberi.[27,28] It is sufficiently accurate to simplify Alberi's formalism slightly and obtain the usual expression[7,9]:

$$\frac{d\sigma}{d\Omega}(K^+d\rightarrow K^+n(p))=(|f_{\rm el}|^2+|g_{\rm el}|^2)I\ , \tag{5}$$

$$\frac{d\sigma}{d\Omega}(K^+d\rightarrow K^0p(p))=|f_{\rm ce}|^2(I-J) + |g_{\rm ce}|^2(I-\tfrac{1}{3}J)\ , \tag{6}$$

where $f_{\rm el}=\frac{1}{2}(f_1+f_0)$, $f_{\rm ce}=\frac{1}{2}(f_1-f_0)$ and similarly for $g_{\rm el}$ and $g_{\rm ce}$. In turn, $f_{0,1}$ is the spin-nonflip part of $Z_{0,1}$, and $g_{0,1}$ is the spin-flip part of $Z_{0,1}$. $I$ and $J$ are functions of energy and scattering angle and have been calculated using the Reid soft-core deuterium wave function.[29] No approximations have been made in their numerical

TABLE II. Data used in the analysis.

| | Type of data | Ref. | Number of momenta (data number) | Laboratory momentum range (GeV/$c$) |
|---|---|---|---|---|
| A. | $K_L^0 p \to K_S^0 p$ | 11 | 1 (19) | 0.550 |
| | differential cross section | 12 | 12 (224) | 0.470–0.790 |
| | | 13 | 9 (169) | 0.650–1.200 |
| B. | $K^+ n \to K^+ n$ polarization | 14 | 4 (36) | 0.851–1.193 |
| C. | $K^+ n \to K^0 p$ polarization | 26 | 1 (5) | 0.600 |
| | | 15 | 4 (32) | 0.851–1.193 |
| D. | $I=0$ total cross section | 16 | 2 (2) | 1.141–1.191 |
| | | 17 | 19 (19) | 0.412–1.065 |
| E. | $I=0$ | | | |
| | total inelastic cross section | 18 | 9 (9) | 0.640–1.210 |
| F. | $K^+ n \to K^+ n$ | 19 | 9 (153) | 0.640–1.210 |
| | differential cross section | 20[a] | 7 (75) | 0.434–0.936 |
| G. | $K^+ n \to K^0 p$ | 21 | 4 (32) | 0.252–0.587 |
| | differential cross section | 22 | 3 (54) | 0.690–0.890 |
| | | 23 | 9 (162) | 0.640–1.210 |
| | | 24 | 3 (54) | 0.865–1.210 |
| | | 20[a] | 7 (114) | 0.434–0.936 |
| H. | $K_L^0 p \to K^+ n$ | | | |
| | differential cross section | 25 | 6 (83) | 0.650–1.150 |

[a]Data starred were not used.

calculation other than those inherent in Alberi's theoretical work.

Appropriate spectator-momentum cuts have been imposed on the calculation of form factors for each data set. We find that, at a given energy, $I$ is constant over a wide range of the c.m. scattering angle $\theta^*$ but, in the very backward direction $I$ decreases more than suggested by Ref. 9. Accordingly we have decided that our knowledge of $I$ is not sufficiently reliable for $\cos\theta^* < -0.9$. Our form of $J$ is negative with a slightly greater magnitude than in Ref. 9 over most of the angular range, but the only important uncertainty is in the forward direction where $J$ increases rapidly. Because of this, the data on reaction (2) has not been used for $\cos\theta^* > 0.9$.

We therefore avoid ranges of the c.m. scattering angle where the form factors are less well known.

### C. Treatment of amplitudes other than $Z_0$

The amplitude for reaction (4) may be written as

$$T=\tfrac{1}{4}(Z_1+Z_0-2Y_1)\,. \tag{7}$$

This shows that an analysis of the $K_L^0$ data requires knowledge of $Z_1$ (already required for an analysis of the $K^+n$ data) as well as $Y_1$, the amplitude for elastic $\bar{K}N$ scattering with $I=1$.

The determination of $Z_1$ from $K^+p$ elastic scattering is relatively straightforward.[6–8] $Y_1$ is determined mainly from $K^-p$ data but in this case $Y_0$, the corresponding amplitude for $I=0$, must also be intoduced.[30,31] An analysis in which all four amplitudes $Z_1$, $Z_0$, $Y_1$, and $Y_0$ were allowed to vary would involve an extremely large data set and many problems of resonance interpretation. Even if desirable in principle, such an analysis represents a forbidding task. In the present work we take the view that $Z_1$ and $Y_1$ are relatively well known (certainly in comparison with $Z_0$) and therefore that it makes sense to fix them in order to fit $Z_0$. This assumption can be checked to some extent by comparing results for $Z_0$ obtained with $Z_1$ and $Y_1$ fixed at different solutions. Despite differences in interpretation of the most recent $Z_1$ analyses,[7,8] we find that the $Z_0$ amplitude obtained, scarcely depends on which form for $Z_1$ is used as input. The $Z_0$ solution is also relatively

insensitive to the choice of $Y_1$. These findings will be discussed in detail in Sec. II F.

Our strategy is to use only those features of the fitted $Z_0$ amplitude which are approximately independent of the $Z_1$ and $Y_1$ input solutions.

### D. Parametrization of the partial-wave amplitudes

The form chosen for the $Z_0$ partial-wave amplitudes was similar to one that was successful in an earlier analysis of elastic $K^+p$ scattering.[6] As well as being explicitly unitary, this parametrization provides an acceptable behavior for the phase shift as $q\to 0$. However, this behavior is not built in at higher momenta. Each partial-wave amplitude is written as

$$T=(\eta e^{2i\delta}-1)/2i \ , \tag{8}$$

where $\delta$ and $\eta$ are parametrized as functions of energy.

For c.m. momentum $q$ above the inelastic threshold $q_0$ (0.305 GeV/$c$), we define $u=(q-\bar{q})/\Delta q$ where $\bar{q}$ is the mean c.m. momentum (0.5 GeV/$c$) with the half-width $\Delta q$ (0.2 GeV/$c$). The phase shift $\delta$ is written

$$\delta(q)=\sum_{m=0}^{M} a_m P_m(u) \ , \tag{9}$$

where $P_m$ is the Legendre polynomial of order $m$ and the $a_m$ are parameters to be determined in the fit. To insure unitarity, the inelasticity $\eta$ is written

$$\eta=1/(1+X^2) \ , \tag{10}$$

where we use the quantity $u_0=(q_0-\bar{q})/\Delta q$ to define $X$:

$$X(q)=\sum_{n=1}^{N} b_n[P_n(u)-P_n(u_0)] \ . \tag{11}$$

The $b_n$ are parameters to be determined by the fit. This form for $X$ automatically vanishes at $q=q_0$ thus giving a smooth onset of inelasticity. The limits $M$ and $N$ in (9) and (11), respectively, were chosen according to the partial wave as follows:

| Wave | $M$ | $N$ |
|---|---|---|
| $S_1,P_1,P_3$ | 3 | 3 |
| $D_3,D_5,F_5$ | 2 | 2 |
| $F_7,G_7,G_9$ | 1 | 1 |

For c.m. momentum below the inelastic threshold, we write

$$\tan\delta(q)=sq^{2l+1} \ , \tag{12}$$

where $l$ is the orbital angular momentum of the partial wave. The quantity $s$ is determined by the parameters $a_m$ via continuity at $q=q_0$. Explicitly we have

$$s=\tan\delta_0/{q_0}^{2l+1} \ , \tag{13}$$

where

$$\delta_0=\delta(q_0)=\sum_{m=0}^{M} a_m P_m(u_0) \ . \tag{14}$$

Finally, of course, we have $\eta=1$ in this case.

Table II shows that the great majority of data used in the present analysis were taken above the inelastic threshold and that the remainder were taken only just below it, so that the conjectured form of $\delta$ in (12) plays a relatively unimportant role.

A comparison can be made of the final fit for the three highest partial waves with the values calculated by Alcock and Cottingham[32]; it is quite successful.

### E. Fitting procedures

To obtain starting points for the minimizations of $\chi^2$, we fitted previously known $Z_0$ solutions from Refs. 7 and 9 to the parametrization described in Sec. II D. This exercise provided a warning that a feature of a partial-wave amplitude found with one parametrization may be difficult or impossible to describe with another. In particular, the fit of Ref. 7 was difficult to characterize in our parametrization. The general question of the sensitivity of our results to the choice of parametrization will be discussed in the next section.

All of the data sets are subject to systematic normalization errors. To allow for these, all data within a given set are divided by a normalization parameter, $N$, which is allowed to vary in the fit but which is constrained to lie close to unity by including an extra term in the $\chi^2$ of the form $[(N-1)/\Delta N]^2$, where $\Delta N$ is the quoted systematic error of the experiment. Thus, for example, all the values of the total cross section produced by one experiment are assumed to have a common systematic uncertainty in addition to their statistical errors. The values of $d\sigma/d\Omega$ for a given reaction

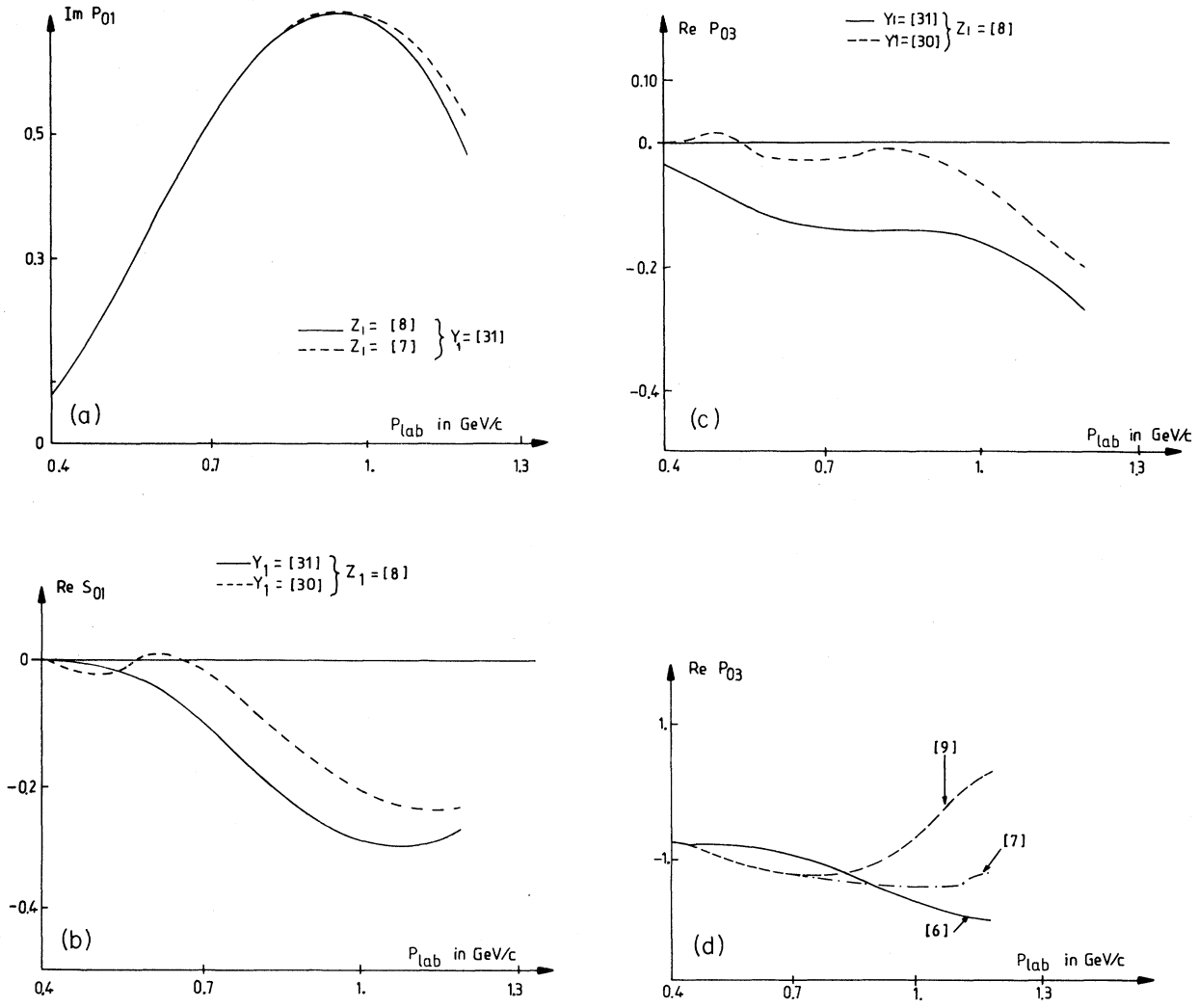


FIG. 1. Sensitivity of $Z_0$ partial-wave amplitudes to various inputs, a worst-case presentation. (a) variation with $Z_1$, (b) and (c) variations with $Y_1$, and (d) variation with parametrization. In all cases the solid curve represents our preferred solution (see later in text).

TABLE III. Parameters of preferred solution for $Z_0$ (see text).

| Partial wave | $a_0$ | $a_1$ | $a_2$ | $a_3$ | $b_1$ | $b_2$ | $b_3$ |
|---|---|---|---|---|---|---|---|
| $S_1$ | −0.1342 | −0.0393 | 0.2956 | 0.1913 | −0.4373 | −0.3544 | −0.0941 |
| $P_1$ | 0.7469 | −0.0885 | −0.4618 | −0.1139 | −0.0003 | 0.0002 | −0.0002 |
| $P_3$ | −0.2051 | −0.2062 | −0.1499 | −0.0749 | −0.0001 | 0.0000 | 0.0000 |
| $D_3$ | 0.2899 | 0.2364 | 0.07657 | | 0.8098 | 0.3088 | |
| $D_5$ | −0.0015 | 0.0923 | 0.0971 | | 0.4423 | 0.2994 | |
| $F_5$ | 0.0691 | 0.1137 | 0.0567 | | 0.4310 | 0.1886 | |
| $F_7$ | −0.0043 | −0.0309 | | | 0.0000 | | |
| $G_7$ | 0.0262 | −0.0087 | | | 0.0951 | | |
| $G_9$ | −0.0254 | −0.0060 | | | 0.0000 | | |

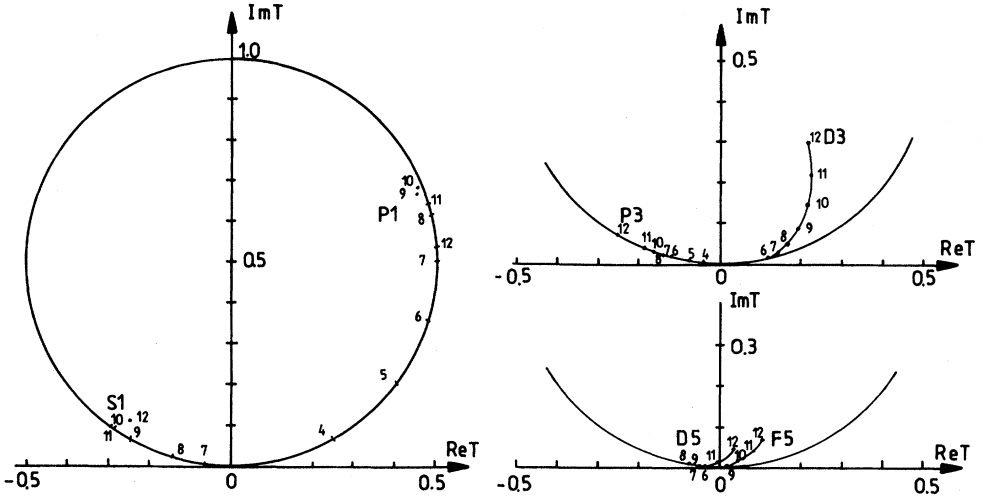


FIG. 2. Argand diagrams showing the $Z_0$ partial-wave amplitudes from the preferred fit described in the text. Points are marked at intervals of 100 MeV/$c$ laboratory momentum. Where necessary to avoid confusion, lower-momentum points have not been marked.

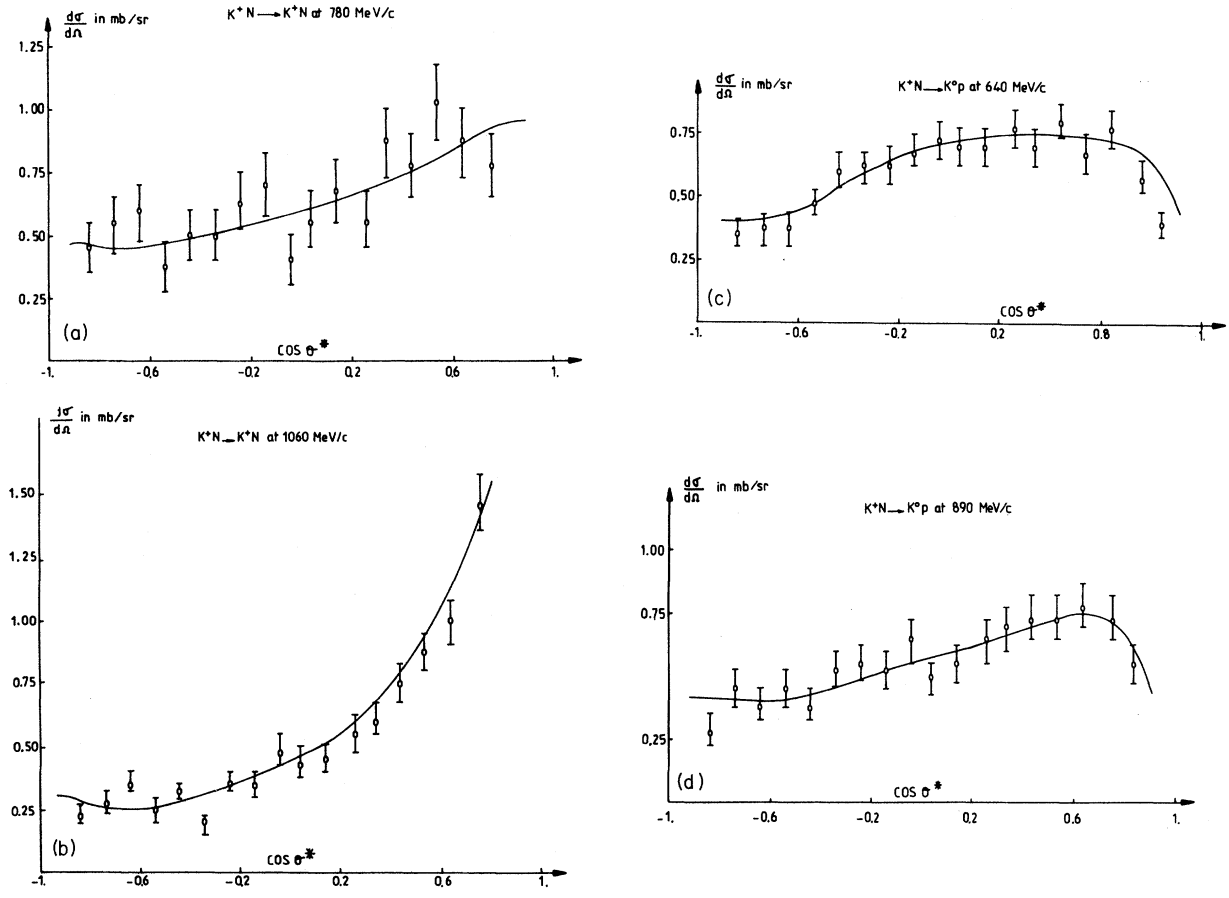


FIG. 3. Sample sets of differential cross sections included in the data set. (a) $K^+n \to K^+n$ at 780 MeV/$c$ (Ref. 19), (b) $K^+n \to K^+n$ at 1060 MeV/$c$ (Ref. 19), (c) $K^+n \to K^0p$ at 640 MeV/$c$ (Ref. 22), and (d) $K^+n \to K^0p$ at 890 MeV/$c$ (Ref. 20). The curves show the predictions of the preferred fit (see later in text).

at a given momentum are treated in a similar way. However we have made the following exceptions to this procedure.

(i) In the case of the Bologna-Glasgow-Rome-Trieste (BGRT) (Ref. 23) measurements of the charge-exchange reaction (2) at nine different momenta, the main normalization error resulted from the determination of the density of deuterium and therefore a single normalization, common to all nine momenta, was used.

(ii) The normalization of the differential cross sections for reaction (3) presented in Ref. 25 is inconsistent with measurements of reaction (2). Hence, only the shapes of the angular distributions were used.

(iii) The shapes and the cross sections for reaction (4) were fitted separately.

Most of the normalization parameters were well behaved in that their fitted values were consistent with unity within the quoted experimental systematic errors. However, those for the $I=0$ total and inelastic cross sections and the cross section for reaction (4) were altered by several standard deviations. To investigate this problem, we carried out a fit with the cross sections for reaction (4) deleted from the data set and found that the normalization parameters for the $I=0$ cross sections were consistent with their quoted experimental errors. Thus the measured $I=0$ cross sections seem to be consistent with the $Z_0$ amplitude extracted from the $K^+d$ data and the angular distributions for reaction (4) but there is clearly a problem in simultaneously fitting the cross section for this reaction. This does not necessarily mean that the data are at fault because it has previously been shown[12] that the overall scale of the $K^0_L p$ cross section is very sensitive to variations in the real part of the $S_1$ wave of the $Y_1$ amplitude; this quantity is not well determined by the $Y_1$ analyses. Hence, in our final analysis, we have fixed at unity the normalization parameters for the $I=0$ total and inelastic cross sections and the $K^0_L p \to K^0_S p$ cross section.

As a general check on analysis procedures, we have compared two independent programs developed at our laboratories. These yield identical results.

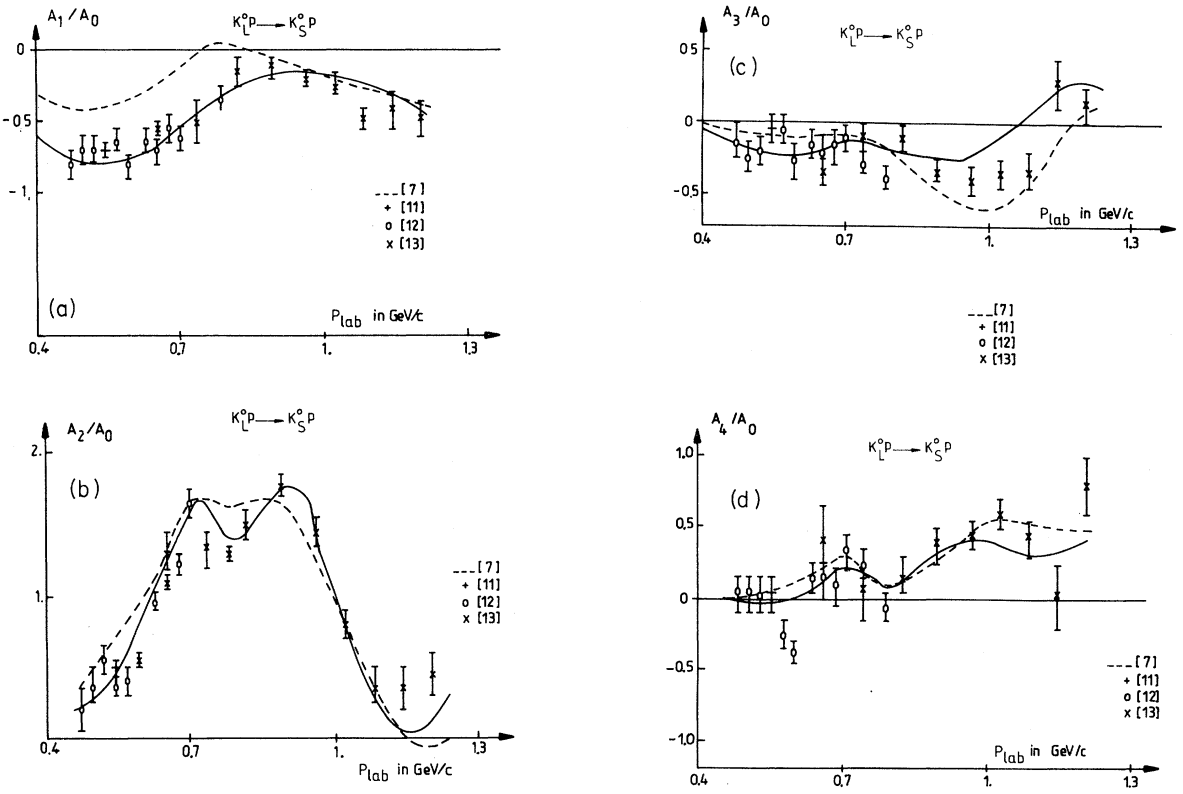


FIG. 4. Legendre-coefficient ratios for the reaction $K^0_L p \to K^0_S p$. Data are taken from Refs. 11–13. The curves show the preferred fit and the predictions of Ref. 7.

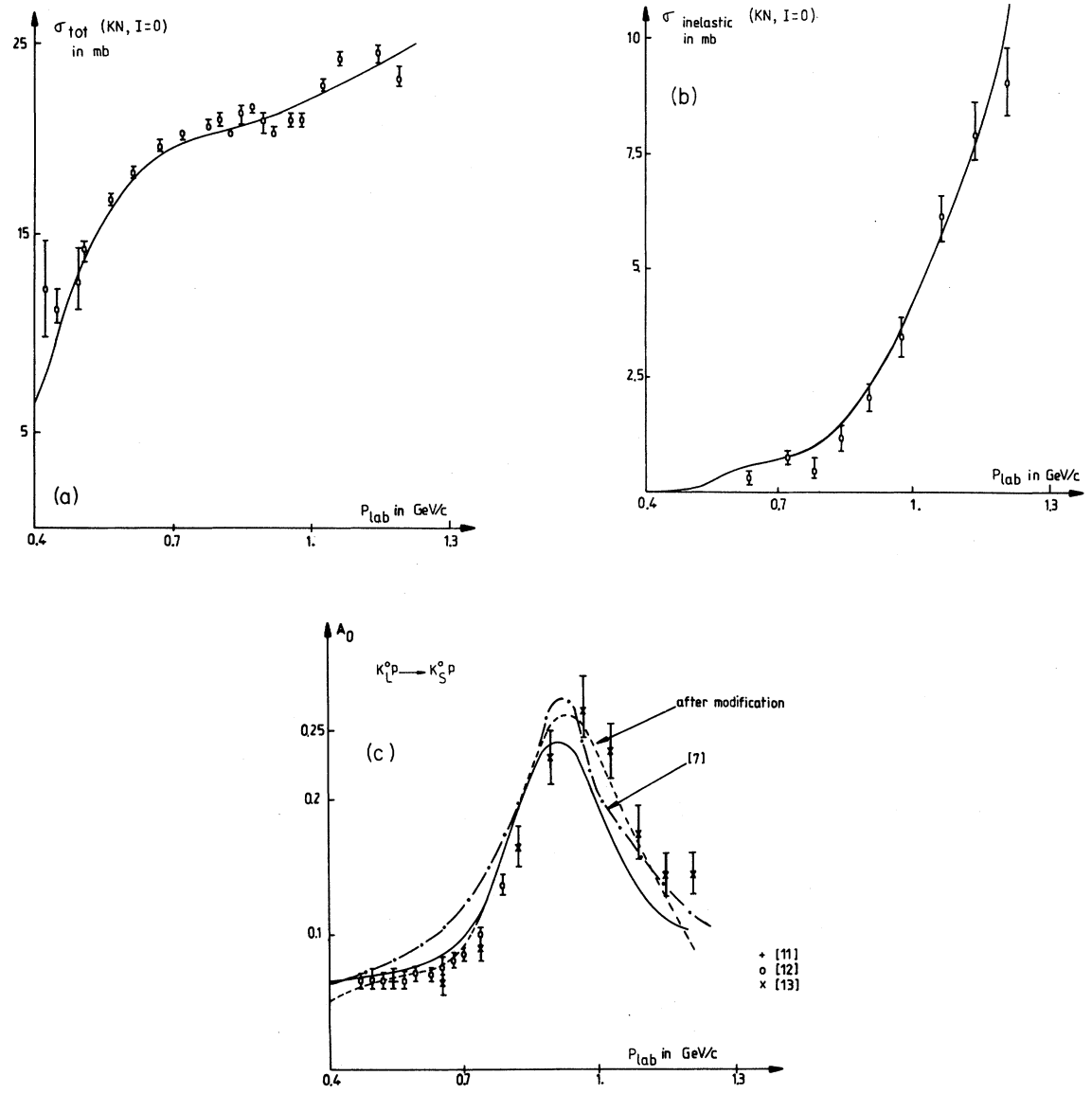


FIG. 5. Cross-section data incorporated in the data set. $\sigma_{\text{tot}}$ and $\sigma_{\text{inel}}$ refer to $I=0$, $KN$ scattering (see Table II for data references) and $A_0$ is for the reaction $K_L^0 p \to K_S^0 p$. In the latter case the data are taken from Refs. 11–13. The continuous curves show the predictions of the preferred fit. The improved fit to $A_0$, obtained by modifying $\text{Re}S_1$ in $Y_1$, is shown by the dashed curve (see Ref. 33). The dot-dash curve is the prediction of Ref. 7.

### F. Sensitivity of our results to inputs

We have studied the sensitivity of the $Z_0$ partial-wave amplitudes to changes in the various inputs involved in the analysis. In each case we have varied one of the standard inputs and compared the resulting fit with our preferred solution (discussed later). To display the differences we present the real and imaginary parts of the partial-wave amplitudes as functions of energy, as applicable.

For reasons of availability of data and computer time, we have used only the data sets (A,D–H) for these studies; this does not alter any conclusion.

First we find that our solution is practically independent of the precise form used for the deuteron form factors. This is only to be expected since we have excluded the regions of the angular distributions where these form factors are most uncertain.

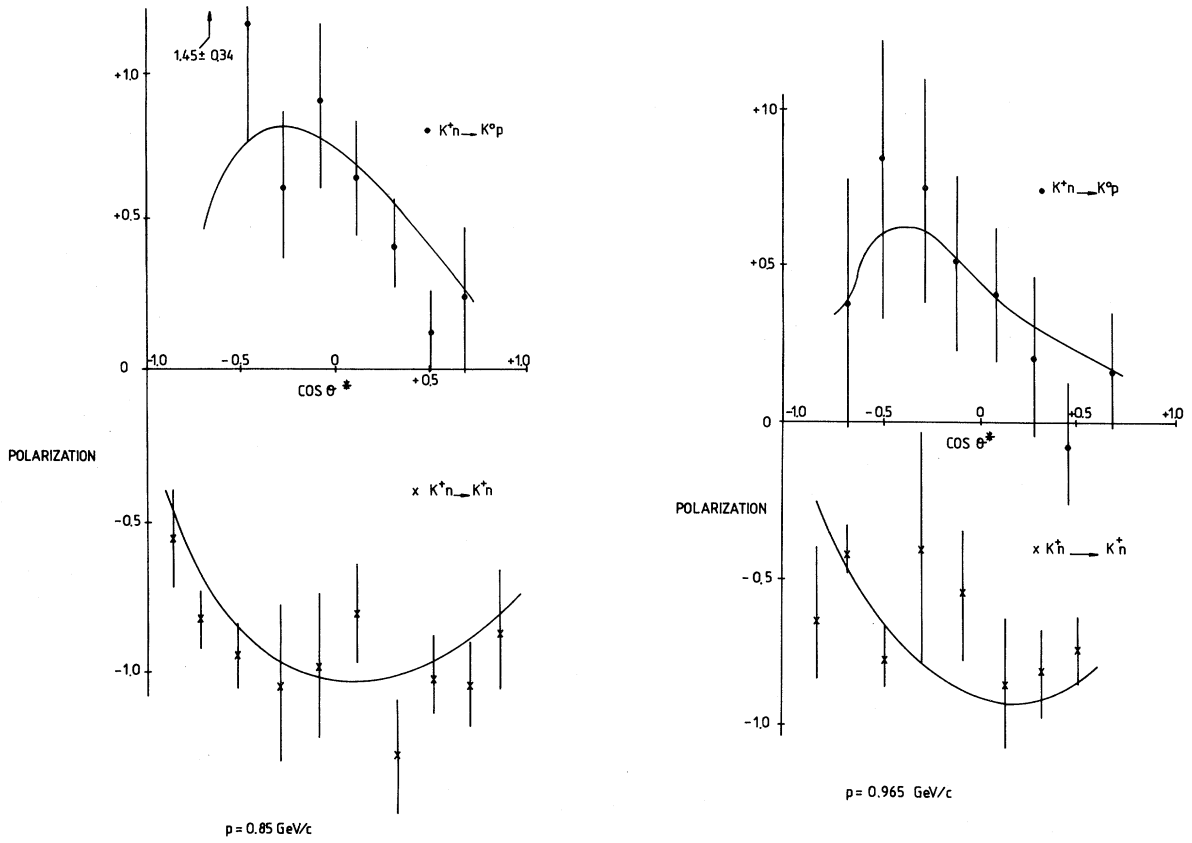


FIG. 6. Polarization as a function of energy and c.m. scattering angle for $K^+n \to K^+n$ and $K^+n \to K^0p$. The curves show the preferred fit.

Second, we have examined the effects of changing the $Z_1$ solution from the most recent solution[8] to that found in Ref. 7. In this case, changes in the partial waves only start to appear at the highest energies studied and all differences are very small. This is gratifying since the $Z_1$ solution[8] that we have used (on the grounds of the data set employed in its determination) contains a somewhat controversial resonance interpretation. We wish to stress that our conclusions are independent of this controversy. For completeness, the biggest difference is shown in Fig. 1(a).

Next the data set has been fitted using a different $Y_1$ solution[30] instead of the most recent one[31] used in our preferred fit. Again most of the partial waves are relatively unaffected but there are some significant changes in $\mathrm{Re}S_1$ and $\mathrm{Re}P_3$ as shown in Figs. 1(b) and 1(c).

Finally we have investigated the sensitivity of our results to the choice of the energy-dependent parametrization for the $Z_0$ partial waves. As alternatives to that described in Sec. II D we have considered the parametrizations used by Martin[7] and by BGRT.[9] Using Martin's parametrization instead of our own, produces very similar partial-wave amplitudes. Using the BGRT parametrization causes a significant change only to the real part of $P_3$, as shown in Fig. 1(d). In any case our parametrization is significantly preferred to the others on the basis of $\chi^2$. These conclusions are unaltered even if we change $Y_1$ and/or $Z_1$.

The sensitivity studies described above show that the basic features of our preferred solution are quasi-independent of the detailed choice of inputs. The few instances where there are significant dependences of any partial wave are shown in Fig. 1.

### G. Results: quasiunique solution for $Z_0$

From the starting values of the previous solutions as well as a large number of alternatives obtained in the course of building up the data set and

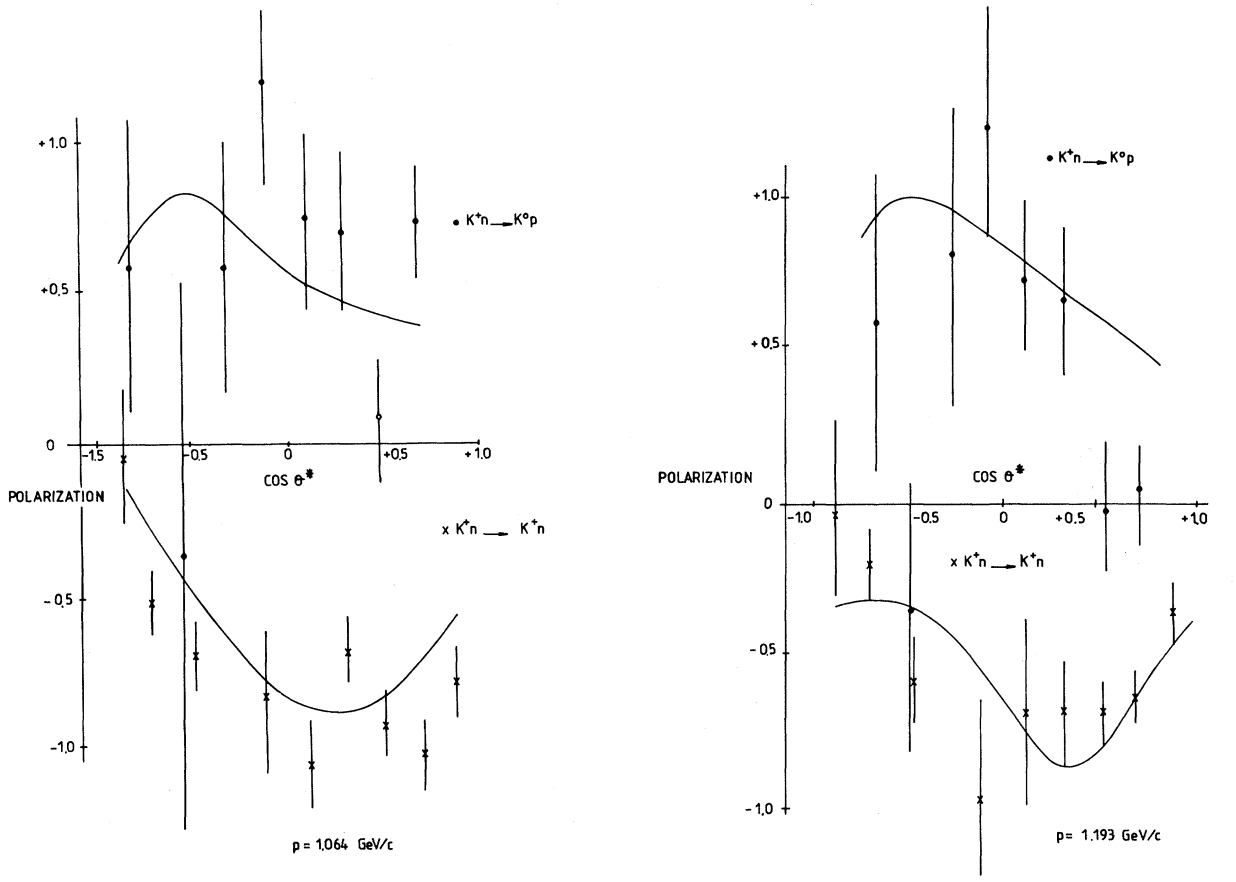


FIG. 6. (*Continued.*)

modifying the parametrization, etc., we have found only two distinct solutions. One of these is analogous to the BGRT A solution and is only found when the fit is started from a point close to that solution. It has a $\chi^2$ which is over 600 more than that of the other solution which is obtained from *all* other starting points. This statistical rejection is due to the new data. Only the second solution with the lower value of $\chi^2$ will be discussed further here.

The parameters of our preferred solution are presented in Table III and Argand diagrams for the partial waves are shown in Fig. 2. This fit has a $\chi^2$ of 1901 for 1156 degrees of freedom. The value of $\chi^2$ could be reduced by about 330 by excluding a few points which seem inconsistent with the rest of the data. However we have not done this because tests have shown that the fitted amplitudes would be scarcely changed. In general, the extensive set of angular distributions for reactions (1) and (2) is described well by the fit and some representative examples are shown in Fig. 3. The comparison with data for reaction (4) is made via the Legendre moments of the angular distribution (Fig. 4) even though the angular distributions themselves were fitted. The predictions of Ref. 7 are also shown. All of the cross-section data that have been fitted are shown in Fig. 5. As discussed earlier the agreement in this case is less good, especially for the cross section for reaction (4).[33] The comparison with the polarization data is shown in Fig. 6. Table IV gives a breakdown of the contributions to $\chi^2$ from the different types of data. We note the large amount of new data ($K_L^0$ and polarization) is well fitted; there is only a small contribution from the normalization parameters. Instead of using our highly correlated error matrix to give a quantitative but hard to interpret estimate of our statistical errors, we prefer to refer to the amplitude variations shown in Fig. 1 which give an estimate of the systematic uncertainties which are larger than the statistical.

In comparing our solution with the one found in the most extensive analysis of $K^+$ data,[7] we find

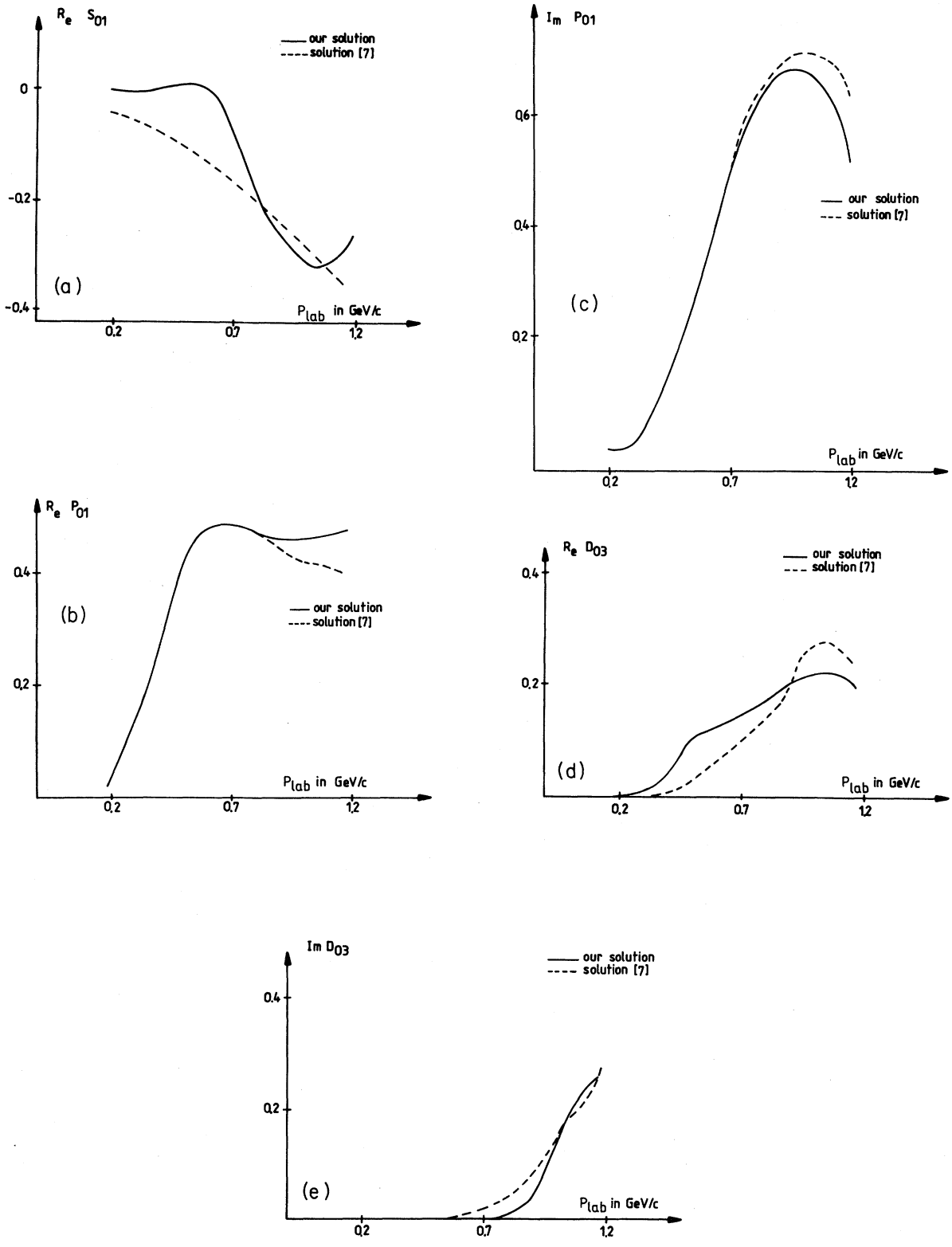


FIG. 7. Comparison of $Z_0$ partial-wave amplitudes found in the present analysis (solid curves) with those found in Ref. 7 (dashed curves).

TABLE IV. Breakdown of $\chi^2$ in final fit in preferred solution.

| Type of data | Number of data | $\chi^2$ |
|---|---|---|
| $I=0$, $\sigma_{\text{total}}$ | 21 | 68 |
| $I=0$, $\sigma_{\text{inelastic}}$ | 9 | 15 |
| $K^+n\to K^+n$, $\frac{d\sigma}{d\Omega}$ | 228 | 347 |
| $K^+n\to K^0p$, $K^0_Lp\to K^+n$, $\frac{d\sigma}{d\Omega}$ | 499 | 682 |
| $K^0_Lp\to K^0_Sp$, $\frac{d\sigma}{d\Omega}$ | 412 | 673 |
| $K^+n\to K^+n$, $\vec{P}$ | 36 | 51 |
| $K^+n\to K^0p$, $\vec{P}$ | 37 | 65 |
| | 1242 | 1901 |

significant differences in $\mathrm{Re}S_1$, $\mathrm{Re}P_1$, $\mathrm{Im}P_1$, $\mathrm{Re}D_3$, and $\mathrm{Im}\ D_3$ which are shown in Fig. 7. This is not surprising since our solution fits the new data quite adequately while the solution of Ref. 7 does not. In addition, our careful analysis of the effects of different parametrization leads to a greater confidence in our solution. To achieve a more satisfactory simultaneous fit to existing $K^+d$ and $K^0_Lp$ data it may be necessary to determine the lower partial waves of the $Y_1$ amplitude more precisely.

## III. DISCUSSION: QUARK AND BAG MODELS

The quasiunique solution for the $Z_0$ amplitude shows no classical resonance behavior in any wave up to center-of-mass energy of 1900 MeV. However one notes (see Fig. 8) the large value (about 60°) for the maximum phase shift for the $P_1$ wave which, in a potential model, is a sign of strong attractive forces.[34]

One has always thought that quark states should manifest themselves as classical resonances in partial-wave analyses, that is, with proper phase shift and speed behavior. However, Jaffe and Low have shown[4] that this is not necessary for most of the multiquark states mainly due to the confinement concept. They have developed a general method which relates the discrete states predicted in a model of confined quarks to hadron-hadron scattering. They introduce a matrix, the $P$ matrix, which connects the interior of the confined region, the "bag", where quarks and gluons are the dynamical variables, and the exterior of this region where the interactions among hadrons are negligible. The eigenstates of the bag model are identified with the poles of the $P$ matrix. The external scattering state is parametrized with the $P$ matrix and is thereby related to the $S$ matrix and thus to the measured phase shifts and elasticities.

We very briefly present the $P$-matrix ideas. For a more thorough discussion, see Refs. 4 and 10. A

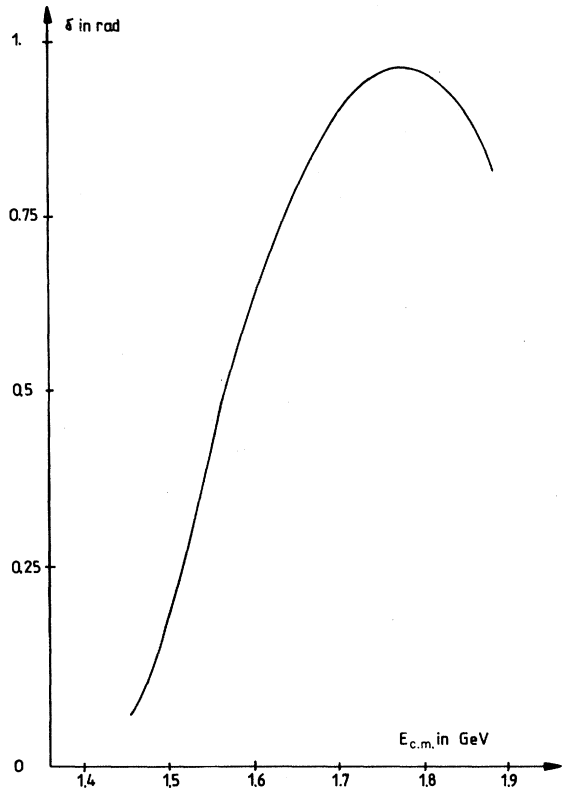


FIG. 8. The $P_1$ phase shift as a function of c.m. energy $W$, in our preferred solution.

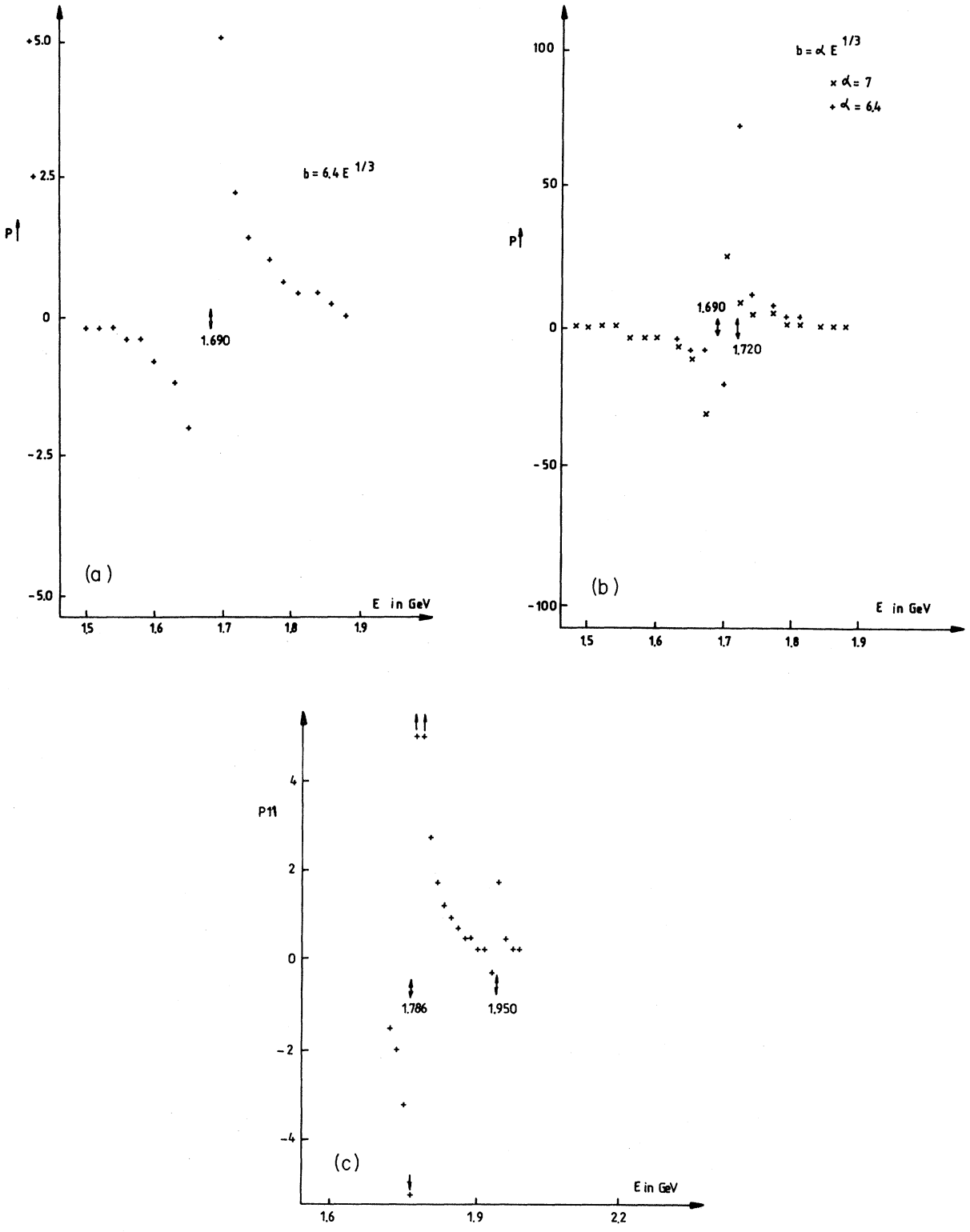


FIG. 9. The $P$ matrix as a function of energy for $I=0$ and (a) $S_1$ wave, (b) $P_1$ wave, and (c) $I=1$, $S_1$ wave (elastic matrix element).

pole in the $P$ matrix corresponds to a state whose wave function vanishes at $r \geq b$, where $b$ is exterior to the interaction region. The relationship between $b$ and the bag radius $R$ is determined as follows for $|q^4\bar{q}\rangle$ state[10]: (1) One calculates the average of the distance squared between the $3q$ and the $q\bar{q}$ pair by using the density function of the five quarks in the spherical bag model. (2) One identifies this average with the average value of $r^2$ obtained from the free meson-nucleon wave function which vanishes for $r=b$.

For $S$-wave meson-nucleon scattering, Roiesnel[10] obtained $b=1.25R$ and, since $R$ is related to the total energy of the bag, i.e., the c.m. energy,

$$b=6.4E^{1/3} . \tag{15}$$

For $P$-wave meson-nucleon scattering, there exists no rigorous formulation of the $P$ matrix. Neglecting spin effects, one can use the formula of Jaffe and Low[4] for meson-*meson* scattering but the conclusions will depend on the relation used between $b$ and $E$. For example when the constant 6.4 in (15) is changed to 7.0, the Jaffe-Low value, pole positions can diminish by 50—100 MeV.

In addition, we must distinguish the $KN$ $I=0$ and $I=1$ analyses since the $I=0$ $KN \to KN\pi$ cross section is negligible up to 1900 MeV while the $I=1$ $KN \to KN\pi$ cross section has a large $K\Delta$ component[35] and a smaller $K^*N$ one. Thus the $I=0$ analysis will use a two-channel $P$ matrix (ignoring the $K^*N$ component).

The $P$ matrix is simply related to the $S$ matrix[4]

$$P_l/kb = \frac{e_l^{-'}(kb) - e_l^{+'}(kb)\bar{S}_l}{e_l^{-} - e_l^{+}\bar{S}_l} , \tag{16}$$

where the $e_l^{\pm}$ are the spherical Bessel functions

$$\bar{S}_l = \frac{1}{\sqrt{k}} S_l \sqrt{k} , \quad S = e^{2i\delta}$$

for the one-channel case and

$$S = \begin{bmatrix} \eta e^{2i\delta_1} & i(1-\eta^2)^{1/2} e^{i(\delta_1+\delta_2)} \\ i(1-\eta^2)^{1/2} e^{i(\delta_1+\delta_2)} & \eta e^{2i\delta_2} \end{bmatrix}$$

for the two-channel case.

For $I=0$ (i.e., single-channel) and $S$ wave, we have evidence (see Fig. 9) for a pole in $P$ at 1.690 GeV. For $P$ wave, we have, ignoring spin effects, evidence for poles (Fig. 9) at 1.720 GeV ($P_1$) and 1.900 GeV ($P_3$) just beyond the range of our analysis. The residues seem reasonable.

For $I=1$ (i.e., two-channel), we use the results of Ref. 8 for the elastic channel and the solution A of Ref. 35 for the $K\Delta$ channel. Solution C has a positive $S$-wave phase shift which is inconsistent with forward dispersion relations, and the inelasticity of the $P_1$ wave of solution B is inconsistent with the analysis of the elastic channel.[36] For the $S$ wave, we have two poles at 1.786 and 1.950 GeV, the latter beyond the range of our analysis (see Fig. 9); the first is consistent with being entirely elastic while the latter has a 13% coupling to the elastic channel. There is a pole in $P_1$ at 1.823 GeV consistent with being entirely elastic and a pole in $P_3$ at 1.788 GeV which is nearly elastic (97%).[37] The residues seem reasonable.

We compare the results of this $P$-matrix analysis with the predictions of Table I. For $Z_0$, the predicted states $S_1(1.700)$, $P_1(1.720)$, and $P_3(1.870)$ correspond closely to the poles found in our analysis. However, the predicted degeneracy $P_1$-$P_3$ is not observed at 1.720 GeV nor at 1.870 GeV. For $Z_1$, the predicted state $S_1(1.900)$ corresponds closely to the pole of our analysis. The predicted degenerate states $P_1$-$P_3$ at 1.870 GeV are perhaps found given our errors but those at 1.910 GeV are not found.[37] It must be noted that these energies are near the edge of our analysis. An important difference between the predictions and the results of our analysis is the pole in $I=1$, $S_1(1.786)$ which is not predicted.

In conclusion, we have presented a partial-wave analysis which has determined a quasiunique amplitude for the $Z_0$ amplitude below 1.89 GeV. This amplitude does not exhibit any classical resonances in any wave. However, a $P$-matrix analysis of the $Z_0$ and $Z_1$ amplitudes demonstrates the existence of a number of poles in $S$ and $P$ waves and thus indicates the presence of primitive multiquark states; there is some agreement with bag-model predictions.

## ACKNOWLEDGMENTS

We are indebted to the authors of Refs. 8, 30, and 32 for communication of their results in detailed numerical form. The Birmingham group also wishes to acknowledge financial support provided by the Science Research Council during the performance of this work. The Paris group would like to thank B. Nicolescu and C. Roiesnel for many illuminating comments.

*Now at Rutherford and Appleton Laboratories, Chilton, United Kingdom.
†Now at Lawrence Berkeley Laboratory, Berkeley, California 94720.

[1]N. Isgur and G. Karl, Phys. Rev. D 20, 1191 (1979).
[2]D. Strottman, Phys. Rev. D 20, 748 (1979); T. DeGrand *et al.*, *ibid.* 12, 2060 (1975).
[3]R. L. Jaffe, Phys. Rev. D 15, 267 (1977).
[4]R. L. Jaffe and F. E. Low, Phys. Rev. D 19, 2105 (1979).
[5]J. J. de Swart *et al.*, in *Baryon 1980,* proceedings of the IVth International Conference on Baryon Resonances, Toronto, edited by N. Isgur (Univ. of Toronto, Toronto, 1981), p. 405; and private communication.
[6]C. J. Adams *et al.*, Nucl. Phys. B66, 36 (1973).
[7]B. R. Martin, Nucl. Phys. B94, 413 (1975).
[8]R. A. Arndt *et al.*, Phys. Rev. D 18, 3278 (1978).
[9]G. Giacomelli *et al.*, Nucl. Phys. B71, 138 (1974).
[10]C. Roiesnel, Phys. Rev. D 20, 1646 (1979).
[11]A. Engler *et al.*, Phys. Rev. D 18, 3061 (1978).
[12]W. Cameron *et al.*, Nucl. Phys. B132, 189 (1978).
[13]M. J. Corden *et al.*, Nucl. Phys. B155, 13 (1979).
[14]A. W. Robertson *et al.*, Phys. Lett. 91B, 465 (1980).
[15]S. J. Watts *et al.*, Phys. Lett. 95B, 323 (1980).
[16]R. L. Cool *et al.*, Phys. Rev. D 1, 1887 (1970).
[17]A. Carroll, *et al.*, Phys. Lett. 45B, 531 (1973).
[18]G. Giacomelli *et al.*, Nucl. Phys. B37, 577 (1972).
[19]G. Giacomelli *et al.*, Nucl. Phys. B56, 346 (1973).
[20]C. J. S. Damerell *et al.*, Nucl. Phys. B94, 374 (1975).
[21]R. Glasser *et al.*, Phys. Rev. D 15, 1200 (1977).
[22]M. Sakitt *et al.*, Phys. Rev. D 15, 1846 (1977).
[23]G. Giacomelli *et al.*, Nucl. Phys. B42, 437 (1972).
[24]A. A. Hirata *et al.*, Nucl. Phys. B30, 157 (1971).
[25]J. C. M. Armitage *et al.*, Nucl. Phys. B123, 11 (1977).
[26]A. K. Ray *et al.*, Phys. Rev. 183, 1183 (1969).
[27]G. Alberi *et al.*, Instituto Nazionale di Fisica Nucleare Report No. INFN/AE-72/3, 1972 (unpublished).
[28]G. Alberi, Instituto Nazionale di Fisica Nucleare Report No. INFN/AE-73/1, 1973 (unpublished).
[29]R. V. Reid, Ann. Phys. (N.Y.) 50, 411 (1968); G. Alberi *et al.*, Phys. Rev. Lett. 34, 503 (1975).
[30]G. P. Gopal *et al.*, Nucl. Phys. B119, 362 (1977).
[31]M. Alston *et al.*, Phys. Rev. D 18, 182 (1978).
[32]J. W. Alcock and W. N. Cottingham, Nucl. Phys. B56, 301 (1973).
[33]To improve the fit, we can use the same arbitrary procedure as (12). We modify the real part of the $S_1$ wave in the $Y_1$ amplitude by adding $\sum_0^4 A_n P_n(x)$, where $1+x=2(P_{\text{lab}}-0.4)/0.81$. We find values ($A_0=0.018$, $A_1=0.055$, $A_2=-0.022$, $A_3=-0.080$, $A_4=-0.105$) which greatly improves the fit to the cross section of (4) (see Fig. 5) but which changes no other conclusions.
[34]J. L. Basdevant, private communication.
[35]G. Giacomelli *et al.*, Nucl. Phys. B110, 67 (1976). The $b$ parameters in Table II were multiplied by $(0.75)^{1/2}$, and for Solution A, $SD1$ wave, the $a$ parameter was changed to $-3.205$ and the $e$ parameter changed sign. We thank F. Rimondi for these corrections.
[36]F. Griffiths, thesis, University of Glasgow, 1971 (unpublished).
[37]By extrapolation of the $I=1$ analysis, we find poles in $P_1$ (2.026 GeV and elasticity 20%) and $P_3$ (1.989 GeV and elasticity 19%), perhaps indicating degenerate states comparable to the prediction at 1.910 GeV.